Journal of Membrane Science & Research

journal homepage: www.msrjournal.com

Research Paper

PES/Quaternized-PES Blend Anion Exchange Membranes: Investigation of Polymer Compatibility and Properties of the Blend

Monaheng L. Masheane [1,2], Arne R. D. Verliefde [2], Sabelo D. Mhlanga [1,*]

[1] *Nanotechnology and Water Sustainability Research Unit, College of Science, Engineering and Technology, University of South Africa, Florida, 1709, Johannesburg, South Africa.*
[2] *Particle and Interfacial Technology Research Unit, Department of Applied Analytical and Physical Chemistry, Faculty of Bioscience Engineering, Ghent University, Coupure Links 653, B-9000 Gent, Belgium*

Article info

Received 2017-11-08
Revised 2018-01-29
Accepted 2018-02-04
Available online 2018-02-04

Keywords

Compatibility
Ion-exchange
Membranes
Polymer blend
Quaternized-polyethersulfone

Highlights

- Investigation of polymer blend compatibility through thermodynamic studies.
- Investigation of membrane formation using cloud point determination technique.
- Synthesis and characterization of ion exchange membranes via phase inversion technique.

Graphical abstract

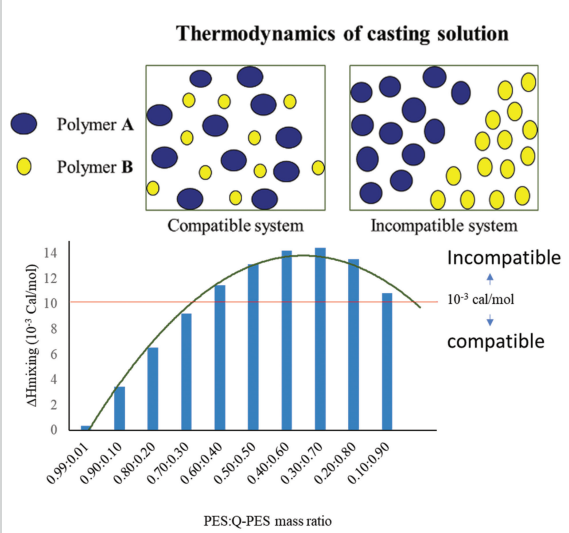

Abstract

Polyethersulfone (PES)-based anion exchange blend membranes were prepared from quaternized-PES (Q-PES) and N-Methyl-2-pyrrolidone (NMP) casting solutions with water as coagulant via non-solvent induced phase inversion. The compatibility of the blend system was investigated through thermodynamic studies while membrane formation was determined using the cloud point technique. The properties of the membranes were investigated using atomic force microscopy (AFM), contact angle measurements and SurPASS Electrokinetic analysis. The ion exchange capacity (IEC) and the swelling of the membranes were also investigated. The PES/Q-PES blend system was compatible at the mass ratio of 0.70:0.30, thus leading to delay in demixing of the solvent and non-solvent during phase inversion. Below 0.70:0.30 mass ratio, the blend system is incompatible, leading to instantaneous demixing of the solvent and non-solvent during the phase inversion process. The roughness and surface charge density increased with the increasing addition of Q-PES while the total surface energy decreased. The IEC increased with the addition of Q-PES while the swelling decreased. Therefore, a suitable compatibility of PES:Q-PES at a mass ratio of 0.70:0.30 and below is the prerequisite for an effective blend system. The conductivity and electrical resistance of the blend membranes were enhanced by the addition of Q-PES additive, while the tensile strength was compromised.

© 2018 MPRL. All rights reserved.

1. Introduction

The development of anion exchange membranes (AEM) for electrolysis, electrodialysis setups, electrodeionisation, electrochemical energy conversion and storage devices (e.g. fuel cell systems) has been a subject of intensive research [1–3]. Ion-exchange membranes (IEMs) suitable for electro-membrane processes should possess the following characteristics [1, 3]:

a) A high ion conductivity that is accomplished by a high ion exchange capacity (IEC), thus low ion resistance and high selectivity.
b) Moderate swelling to compensate for mechanical, thermal and chemical stability.

The main challenge is to develop AEMs with all the desired properties

* Corresponding author at: Phone: +27114712104
E-mail address: mhlansd@unisa.ac.za (S. Mhlanga)

DOI: 10.22079/JMSR.2018.74701.1163

mentioned above, *i.e.* high conductivity, low ion resistance and high IEC, moderate swelling and good thermal, mechanical and chemical stability. One of the viable approaches is to develop AEMs with distinct hydrophobic-hydrophilic separated phase morphology [4]. The hydrophilic ionic segments spontaneously segregate from the hydrophobic matrix to form ionic clusters during the membrane casting process. Ionic clusters with good connectivity induce the formation of hydrophilic channels and facilitate fast ion conduction and water diffusion. Accordingly, AEMs with hydrophilic channels show remarkably higher conductivity than membranes without hydrophilic channels for a given IEC [4, 5].

Different strategies have been reported in the literature for the development of high-performance membranes with reduced swelling and improved IEC, mechanical and chemical properties including grafting, cross-linking and blending. Amongst these techniques, the polymer blend method is the most common and simple method used to modify membrane properties such as the surface charge density, mechanical strength and thermal stability [6]. This is due to its ease of operation, mild environmental conditions used and stable performance. Polymer blending can be done by blending the main polymer with polymers that can form a hydrogen bond. The formation of a hydrogen bond leads to compatibilization of the blend polymer. Blend membranes must have IEC of 0.14 to 0.17 mmol/g and show low ionic resistances for application in electromembranes [7].

The compatibility between the polymers is an important factor that impacts the structure and properties of the blend membrane system. Various types of polymers functionalized with quaternary ammonium groups have been developed and investigated as AEMs. These include poly(arylene ether sulfone), poly(phenylene oxide), poly(ether sulfone), poly(ether ketone), poly(olefin), poly(styrene) and poly(phenylene) [2, 5, 8]. However, there are still some disadvantages in a single polymeric material. Therefore, it is necessary to enhance those properties. Liao and co-workers (2015) fabricated quaternized polysulfone/functionalized montmorillonite nanocomposite membranes and evaluated their potential to be used as IEMs. The quaternized polysulfone (QPSF) has shown enough ionic conductivity at high IEC, but a relatively low mechanical strength because it is difficult to balance the high ionic conductivity and sufficient mechanical properties [9]. Jannasch and coworkers (2014) investigated AEMs based on poly(-sulfone) with 2-4 quaternary ammonium functionalities per benzene ring. Highly localized ionic groups promoted the formation of ionic clustering, which resulted in high conductivity at low water uptake compared with randomly functionalized polymers [10].

Polyethersulfone (PES) is one of the most widely used thermoplastic polymers in membrane separation processes due to its excellent mechanical, thermal and chemical stabilities, as well as environmental endurance and ease of processing. Other desirable properties of PES include creep resistance and inherent flame resistance [11]. However, due to its structure, it has a low IEC and high ionic resistance, which are very important in AEMs. A lot of investigation has focused on modification of PES to enhance those properties. The PES membrane can be blended with polymers possessing quaternary ammonium groups in an attempt to develop AEMs.

To the best of our knowledge, no study has been reported on the investigation of the PES/Q-PES compatibility and the properties of the blend. In the present work, we report the synthesis of PES/Q-PES anion exchange blend membranes using phase inversion. Compatibility and morphology of the membranes were investigated to improve the properties of the membranes. The Schneier theory and ternary diagram were employed to explore the compatibility of the blend system and membrane formation process, respectively [12]. The Shcneier is a theory used to determine the compatibility of the system consisting of two polymers based on the degree of free energy of mixing or heat of mixing. The effect of the polymer blend ratio on the morphology, thermal stability, and mechanical properties was investigated.

2. Experimental

2.1. Materials

Polyethersulfone (PES, MW = 58 kDa), nitric acid (HNO_3, AR grade, 70%), sulfuric acid (H_2SO_4, reagent grade, 95 - 98%), tin (II) chloride ($SnCl_2{\cdot}2H_2O$, ≥ 99.995% trace metals basis) sodium chloride (NaCl), hydrochloric acid (ACS reagent, 37%), N-methyl-2-pyrrolidinone (99%) were obtained from Sigma-Aldrich (South Africa and Germany) and were used as received unless otherwise stated in the synthesis procedure.

2.2. Preparation of quaternized PES

Quaternized-polyethersulfone (Q-PES), also known as aminated-PES (A-PES/NH_2-PES) was synthesized by a two step-process that involved nitration of PES to form nitro-PES (NO_2-PES), followed by nitro-reduction as shown in Figure 1. In a typical nitration reaction, 30 mL of HNO_3 and 40 mL H_2SO_4 were mixed in a 250 mL flask. After cooling, 10 g PES was slowly added into the mixture, and the reaction was continuously stirred at 65 °C for 6 h. The flakes obtained were then washed with deionized water to attain a neutral pH. The product was dried at 70 °C in a DHG Heating Drying Oven for 24 h and then crushed to fine powder to be used in a subsequent reaction [9].

In the nitro-reduction reaction, 0.089 mol $SnCl_2{\cdot}H_2O$ was dissolved in 37% HCl (45 mL), followed by the addition of 50 mL ethanol into the mixture. The mixture was stirred for 15 min, and then NO_2-PES fine power was added step-wise. The final mixture was stirred for 6 h at 65 °C to obtain a yellowish precipitate, which was filtered and washed with deionized water to attain the neutral pH. After drying at 70 °C in the DHG Heating Drying Oven for 24 h, the product was crushed into a fine powder and then characterized and used in the preparation of anion exchange PES-based materials [9]. The degree of quaternization (DQ) was determined using Equation 1:

$$DQ\,(\%) = \frac{W_g - W_o}{W_o} \times 100 \tag{1}$$

where W_g denotes the weight of Q_PES while the W_o is the initial PES weight.

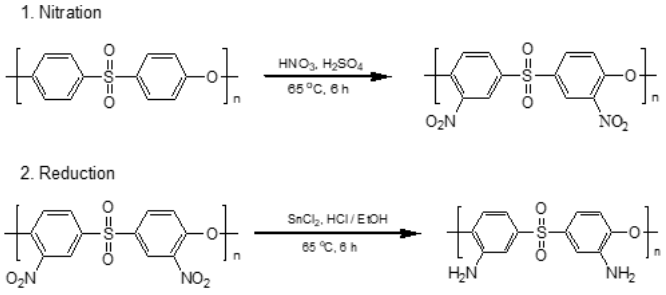

Fig. 1. Schematic illustration of the synthesis of aminated polyethersulfone (Q-PES) from polyethersulfone (PES).

2.3. Determination of polymer blend compatibility

2.3.1. Thermodynamic analysis

A blend solution containing 16% wt of PES/Q-PES, 84% NMP was prepared. The ratios of PES: Q-PES were varied to investigate the compatibility of the blend system. The heat of mixing the blend system can be an estimated presentation of free energy mixing (ΔG_m) (Equation 2) to predict the level of compatibility of polymers. According to thermodynamic theory, the completely compatible system may be formed if $\Delta G_m < 0$,

$$\Delta G_m = \Delta H_m - T\Delta S_m \tag{2}$$

where ΔH_m is enthalpy of mixing, T is the absolute temperature and ΔS_m entropy of mixing. For most of the polymer system, the ΔS_m is small and ΔG_m depends on ΔH_m. Therefore, the effect of decreased ΔH_m would favour the miscibility owing to the decrease in ΔG_m. Schneier (1973) [12] revealed that the blend system compatibility could be estimated through the calculation of ΔH_m (Equation 3) based on the theory of Flory-Huggins. If $\Delta H_m \leq 10\times10^{-3}$ cal/mol the blend system is compatible, otherwise the system is incompatible if $\Delta H_m \geq 10\times10^{-3}$ cal/mol.

$$\Delta H_m = \left\{ X_1 M_1 \rho_1 (\delta_1 - \delta_2)^2 \left[\frac{X_2}{(1-X_2)M_2\rho_2 + (1-X_1)M_1\rho_1} \right] \right\}^{\frac{1}{2}} \tag{3}$$

where X_1 and X_2 is a mass fraction of the polymer $X_1+X_2=1$, M is the molecular weight of the monomer unit (g/mol), ρ is polymer density (g/mol) and δ is the solubility parameter of the polymer (cal/cm^3).

2.3.2. Cloud point determination

The phase diagram of the ternary membrane forming systems (PES/Q-PES-NMP-Water) was determined by visual observation of the turbidity change of the casting solution when titrated with a non-solvent (water) [13]. For this particular experiment, the mass ratio of the PES: Q-PES blend system

was 50:50 wt/wt. Blend polymer casting solutions were weighed before and after the experiment. The casting solution was transferred into a beaker at a constant temperature of 70 ºC. The temperature was maintained at 70 ºC using a water bath and the cloud points were measured at this temperature by slowly adding distilled water into the blend polymer casting solution using a syringe. This was done until the clear blend polymer solution turned to a cloudy solution. Then, the cloud points were reached when the turbidity of the blend casting solution did not change anymore after 24 h of stirring. The composition of the cloud points was calculated by the amount of non-solvent (water), solvent (NMP) and polymer blend (PES/Q-PES).

2.4. Preparation of the blend membranes

PES/Q-PES blend membranes were fabricated using a phase inversion method, also known as immersion precipitation/coagulation [14] using a blend solution containing 16% wt of PES/Q-PES, 84% NMP. The ratios of PES:Q-PES were varied in the range where the polymers are compatible. The compositions of the casting solutions for the prepared membranes are reported in Table 1.

Table 1
Composition of the casting solutions used in the preparation of blend membranes.

Sample name	PES:Q-PES (wt/wt)	PES (%)	Q-PES (%)	NMP (%)
M0	1.00:0.00	16.00	0.00	84
M1	0.99:0.01	15.84	0.16	84
M2	0.90:0.10	14.40	1.60	84
M3	0.80:0.20	12.80	3.20	84
M4	0.70:0.30	11.20	4.80	84

Typically, different mass ratios (w/w%) of polymers were dissolved in NMP and mixed thoroughly under constant mechanical stirring at 30 ºC until homogeneous mixtures were formed. The homogeneous solutions were degassed to remove bubbles. Thereafter, the prepared solutions were cast on a smooth glass plate substrate at room temperature using a casting knife (Elcometer 3545 Adjustable Bird Film applicator) with a gap of 250 µm. Subsequently, the substrate glass plates were horizontally immersed in a coagulation bath containing distilled water, which induced phase inversion. The prepared membranes were stored in another water precipitation bath for 24 h to ensure complete phase separation. Finally, the prepared membranes were removed from the coagulation bath and then sandwiched between paper towels at room temperature for drying. The thickness of the membranes was measured using a micrometer.

2.5. Characterization of the Q-PES polymer

The structure of Q-PES was confirmed using ^{1}H NMR Bruker Avance II 400 NMR spectrometer at the resonance frequency of 400 MHz, using DMSO-d_6 as a solvent and tetramethylsilane as an internal standard. Typically, about 3 %(w/v) of PES, PES-NO_2 and Q-PES polymers were dissolved in DMSO-d_6 and then loaded in an NMR spectrometer at 60 ºC. The functional groups of the synthesized Q-PES were determined using the Perkin Elmer 100 Fourier transform infrared-attenuated total reflectance (FTIR-ATR) spectrometer. The samples were cut into small pieces and placed on the ATR while scanned in wavenumbers between 500 and 4000 cm^{-1} at the spectral resolution of 4 cm^{-1}.

2.6. Characterization of the membranes

2.6.1. Surface morphology of the membranes

The surface topology of the membranes was characterized using atomic force microscopy (AFM) (WITec AFM alpha300 A). Approximately 1 cm^2 of the membrane samples were fixed on a specimen holder and 4 µm × 4 µm of the area was scanned in a non-contact mode and high resolution to minimize membrane surface damage. The surface roughness parameters were reflected in terms of the average roughness (S_a), the root mean square of the Z data (S_q) and the mean difference between the highest peaks and the lowest valleys (S_z).

2.6.2. Charge density of the membranes

The membrane surface charge properties were measured using a streaming potential method. A SurPASS Electrokinetic Analyzer (Anton Paar Gmb) was employed for this experiment. The measurements were carried out with 0.001 M aqueous KCl solution adjusted to the desired pH with HCl or NaOH solution. The zeta potential was given by the Helmholtz–Smoluchowski equation with the Fairbrother and Mastin approach (Equation 4) [15]:

$$\xi = \frac{\Delta E \eta k}{\Delta P \varepsilon \varepsilon_o} \tag{4}$$

where ξ is the zeta potential, ΔE is the streaming potential, ΔP is the applied pressure, η is the viscosity of the solution, k is the solution conductivity, ε and ε_0 are the permittivity of the test solution and free space, respectively.

2.6.3. Thermal stability of the membranes

Thermal properties of the bare PES and the blends were studied using a Perkin Elmer 4000 thermogravimetric analyzer (TGA). The materials were initially vacuum dried at 50 ºC for 24 h, equilibrated at 30 ºC and then heated to 800 ºC at a heating rate of 10 ºC min^{-1} under nitrogen (N_2) flow. The derivative thermogravimetry (DTG) curves were calculated by the first order differential of the respective TGA curves over temperature.

2.6.4. Contact angle measurements and surface free energy of the membranes

The wettability of the surface films of membranes was characterized by measuring the contact angles of water, glycerol, and diiodomethane (DDM) using the sessile drop method. A Data Physics contact angle OCA 15 EC GOP equipped with a computer controlled video camera was used to measure these contact angles. About 5 µL of each of the solvents from a syringe was carefully dropped onto the surface of the membranes. The solvent droplet image in contact with the membrane surface was captured using the video camera and the contact angle was determined [14]. To minimize the experimental error, the contact angle of each of the membranes for each of the solvents was measured at 10 random locations and the average value was reported.

The contact angle values were used further to calculate the total surface free energy at the interface between the liquid and the surface of the membranes (γ_s^T). There are several approaches for determination of the γ_s^T and its components. Chibowski proposed the quantitative description of the interactions of the solvents with the membrane surface using Equation 5 [16].

$$\gamma_s = \gamma_L(1+\cos\theta) \tag{5}$$

where γ_L is the surface tension of the probe liquid and θ is the contact angle. The values γ_s are apparent resulting from the interactions present on the solid/liquid interface which include van der Waals interactions and hydrogen bonds [17].

According to the van Oss and co-workers (1988) approach, the total surface free energy can be divided into two components [18]. These are the Lifshitz-van der Waals (or polar) component (γ_s^{LW}) involving the dispersion, induction (Debye) and dipole (Keesom) contributions; and the Lewis acid-base (or polar) components (γ_s^{AB}) (Equation 6) [17].

$$\gamma_S^T = \gamma_S^{LW} + \gamma_S^{AB} \tag{6}$$

Van Oss et al. suggested that electron-donor (Lewis base) and electron (Lewis acid) interactions are normally quite different and play different roles in the interfacial interactions [18]. These are therefore described accordingly by two distinct parameters, which are electron-donor (γ_s^-) and an electron acceptor γ_s^+, contrary γ_s^{LW} (Equation 7).

$$\gamma_S^{AB} = 2\sqrt{\gamma_S^-\gamma_S^+} \tag{7}$$

The principal polar interaction is hydrogen bonding, involving donors and acceptors; hence the polar interactions justify the dual nature of such interactions. Nevertheless, they are not limited to hydrogen bonding but include all electron-donating and electron-accepting phenomena. Based on this model, the work of adhesion (W_A^a) between liquid and solid can be expressed as the Oss-Chaudhury- Good equation (Equation 8) [18, 19]:

$$W_A^a = \gamma_L(1+\cos\theta) = 2\left(\sqrt{\gamma_S^{LW}\gamma_L^{LW}} + \sqrt{\gamma_S^+\gamma_L^-} + \sqrt{\gamma_S^-\gamma_L^+}\right) \tag{8}$$

When the contact angle measurements are contacted with an apolar liquid, i.e. DDM with a known γ_L and γ_L^{LW} which are equal due to the fact the γ_L^+ and γ_L^- are equal to zero [19], Equation 7 is reduced to Equation 9:

$$\gamma_L(1+\cos\theta) = 2\left(\sqrt{\gamma_S^{LW}\gamma_L^{LW}}\right) \quad (9)$$

2.6.5. Water uptake and IEC

The water uptake was determined using a dry-wet weight method. Generally, the membrane samples were immersed in deionized water for 48 h at room temperature, and the excess water was removed by wiping the surface of the membranes with a paper towel. Then the membranes were weighed by using an analytical balance. Subsequently, the wet membrane samples were dried in a DHG Heating Drying Oven at 45ºC for 24 h and weighed. Water uptake (Φ) was expressed as

$$\%\Phi = \frac{W_w - W_d}{W_d} \times 100 \quad (10)$$

where W_w and W_d are weights in g of wet and dry membranes, respectively, d_w is the density of water (0.998 g/cm^3), A is the membrane effective area (m^2) and l is membrane thickness.

The IEC of the membranes was determined by the definitive Mohr method. Typically, the membrane samples were equilibrated in 1.0M NaCl solution for 24 h in order to convert all charged sites to the chloride ion (Cl^-) form. Then, the excess NaCl was removed by washing the membrane samples with deionized water. The Cl^- form membrane samples were further equilibrated with 0.5 $NaNO_3$ for 24 h. The liberated Cl^- ions were determined by titration with 0.05 M $AgNO_3$ using K_2CrO_4 as an indicator. The IEC (mmol·g^{-1}) was calculated using Equation 11 [20]:

$$IEC = \frac{C_{AgNO_3} V_{AgNO_3}}{W_d} \quad (11)$$

2.6.6. Electrical resistance and conductivity of the membranes

Q-PES/PES blend membranes were equilibrated in 0.5 M NaCl and then placed in a two-compartment cell (made of Pyrex glass) between two platinum electrodes with effective areas of 1 cm^2. The resistance of the membranes was measured at room temperature using impedance spectroscopy (IS) in the frequency of 10^6 Hz with an oscillating voltage of 100 mV amplitude. The membrane resistance (R_m (Ω)) was calculated using different resistance between the cell (R_1) and the electrolyte solution (R_2) ($R_m = R_1 - R_2$). The membrane areal resistance, r (Ω cm^{-1}) was expressed as follows:

$$r = R_m A \quad (12)$$

where A is the area of the membrane (cm^{-2}). Based on the electrical resistance of the membranes, the conductivity, σ (S cm^{-1}) of the membranes was determined using Equation 5.

$$\sigma = \frac{L}{r} \quad (13)$$

where L is the thickness of the membranes.

2.6.7. Tensile strength

The tensile strength of the membranes was determined using Small Angle X-ray Scattering (SAXspace) Anton Paar installed with an ST600 tensile stage of 600 N load cell.

3. Results and discussion

3.1. Characteristics of Q-PES

3.1.1. Physical properties synthesized of Q-PES

In this study, the aminated-PES (or Q-PES) with 89% degree of quaternization was synthesized using a two-step process, which involves nitration of pristine-PES to form PES-NO_2 and the ultimate reduction of nitro functional groups to amines (Q-PES). Upon the nitration process, the white powdered pristine PES (Figure 2A) was changed to yellow flakes (Figure 2B). These flakes were then transformed into a brownish powder (Figure 2C).

3.1.2. Structure and functional groups of Q-PES

Figure 3 shows the ^{1}H NMR spectra of PES and Q-PES. For PES, there were two distinct peaks which indicated the aromatic ring. The up-field doublet peak represents hydrogen (H_b) at ortho-position to the alkoxyl group, while the down-field doublet peak represents hydrogen (H_a) at ortho-position to sulfonyl group in PES (Figure 3A). There was an introduction of nitro group onto the aromatic ring after nitration. This was represented by a down-field single-peak at δ=8.68 ppm (Figure 3B). This down-field shift is attributed to the presence of aromatic proton (H_c) at ortho-position of two highly electron withdrawing sulfonyl and nitro groups. The presence of some additional peaks in the spectrum was credited to the presence of nitro group on the aromatic ring, which resulted in shifting of δ-values. After the reduction of PES-NO_2 to Q-PES, ^{1}H NMR revealed the presence of an aryl-NH_2 group (Figure 3C). This was shown by a singlet-peak of the amino group at δ=5.7 ppm and the singlet-peak at δ=8.68 (H_c) in PES-NO_2 (Figure 3B) was shifted to δ=8.33 (H_d) due to the electron withdrawing nature of the amino group.

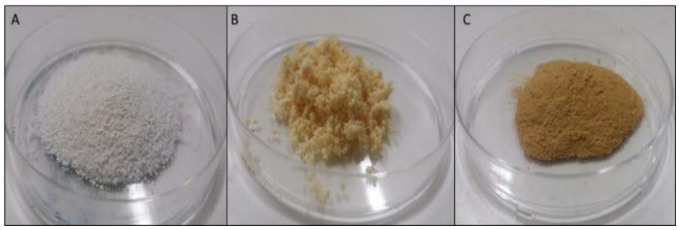

Fig. 2. Pictures of PES (A), PES-NO_2 (B) and Q-PES.

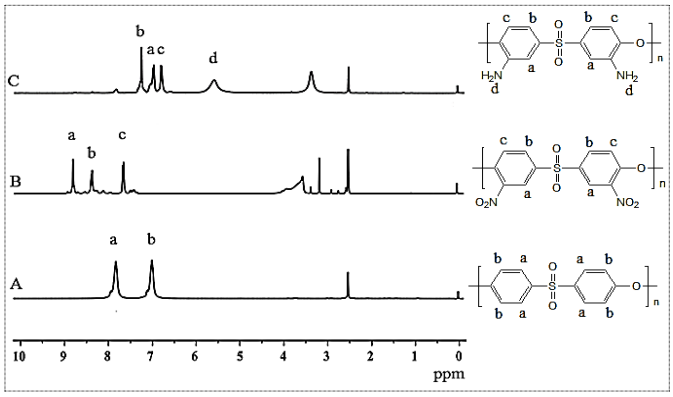

Fig. 3. ^{1}H NMR spectra of PES (A), PES-NO_2 (B) and Q-PES (C).

The molecular structure and the presence of functional groups on the PES polymer were affirmed by FT-IR spectroscopy (Figure 4). Spectrum (A) confirms the characteristics peaks of the pure PES structure. This molecular structure comprises a benzene ring, a sulfone and ether bond. The small peak at ~3079.2 cm^{-1} was attributed to C-H stretching peak of the benzene ring. Two peaks of aromatic skeletal vibrations were observed at 1534.7 and 1420.3 cm^{-1}. The characteristic adsorption band of the aromatic sulfone group was observed at 1143.7 cm^{-1}, while the peak for aryl oxide was found at 1236.6 cm^{-1}.

Figure 4B spectrum shows the same characteristic peaks as PES. The new peaks at 1531.3, 1138.5 and 877.1 cm^{-1} were attributed to asymmetric stretching vibration of - NO_2, the symmetric vibration of -NO_2, and C-N stretching, respectively. This suggests the successful attachment of NO_2 onto the molecular structure of the PES polymer. The attachment of -NH_2 onto the PES molecular structure is observed on the spectrum (C). This was based on the appearance of 3345.4 and 1609.5 c m^{-1}, which was assigned to asymmetrical and symmetrical stretching vibrations of -NH_2, and the peak at 1280.6 cm^{-1} was attributed to C - N stretching. Scheme 2 illustrates the attachment of NO_2 and NH_2 on the surface of PES.

3.1.3. Thermal stability of Q-PES

The thermal stability of the membranes was studied using thermogravimetric analysis (TGA) and the results are depicted in Figure 5. It is revealed that bare PES showed good thermal stability at high temperature in the air. The bare PES completely degraded at a temperature around 580ºC. Both nitro- and Q-PES exhibited significant mass loss in three steps that were due to water loss and loss of sulfone (first loss), nitro and amide groups (second loss) [14], as well as degradation of the polymer chain (third loss).

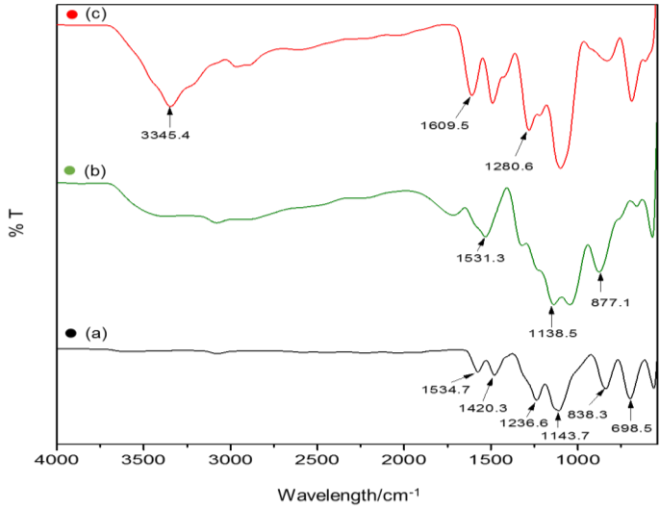

Fig. 4. FTIR spectra of pristine PES (a), PES-NO_2 (b) and Q-PES (c).

3.2. Determination of polymer blend compatibility

3.2.1. Thermodynamic analysis: compatibility

The compatibility between PES and Q-PES polymers was determined using the Schneier theory. The polymer parameters are shown in Table 2, and the ΔH of mixing of different blends of the polymers (PES/Q-PES) were calculated from Equation 1 and presented in Figure 6. ΔH values of the blends solely depend on the composition. When the ratio of PES:Q-PES was less than 0.80:0.20 wt/wt, the ΔH_m values of the blends were less than 10×10^{-3} cal/mol. This suggested that the blend systems of PES:Q-PES were compatible below that mass ratio. However, in the ratio range of 0.80:0.20 wt/wt and above, the values of ΔH of the blend were greater than 10×10^{-3} cal/mol. This indicated that the blend systems were incompatible in that instance (Figure 6). This meant that the PES/Q-PES blends showed heterogeneous behaviour with a strong repulsive force between the two types of hydrophobic macromolecule materials. Thus, the hydrophobic macromolecule of Q-PES was covered by hydrophobic PES matrixes, which resulted in their difficulty in connecting with each other. However, the strong interactions between PES chains dominated over the poor interactions between Q-PES chains when the number of hydrophobic macromolecules was low; that is, the connection between PES chains played a primary role rather than Q-PES. On the other hand, a connection between PES clusters would be formed by increasing the concentration of Q-PES in the blend polymer system, leading to the formation of the incompatible mixture. Generally, the PES/Q-PES blend system is compatible at a certain mass ratio range and incompatible at some mass ratio. Therefore, the compatible system can only be achieved by careful control of the amount of each polymer blended with the other.

Table 2
The density, molecular weight and solubility parameters of the PES and Q-PES polymer.

Polymer	Density g/ml	Molecular weight g/mol	Solubility/ $(cal/cm^3)^{1/2}$
PES	1.44	232	11
Q-PES	1.33	262	10

3.2.2. Cloud point determination

The determination of the cloud point is the most simple and common used method for characterization of the thermodynamics of the systems. By plotting the cloud points, a curve is obtained that borders stable polymer solutions from meta- and unstable compositions [13]. In the ternary system, which is the system in which the polymer is monodispersed, the cloud-point curve coincides with the bimodal, the line that represents the compositions that are in a different phase but in equilibrium with each other. However, in a quasi-ternary system, in which the polymer is poly-dispersed (this is the scenario for most of the commercial bulk polymers used in the preparation of the membranes), the polymer becomes fractionated at equilibrium between the two phases. The lower-fractions prefer the polymer-lean phase, while the higher fractions are mainly present in the polymer-rich phase. This means the polymer-rich phase in equilibrium with polymer-lean phase will not lie exactly on the bimodal and the polymer-lean will also not be located exactly on the bimodal [21].

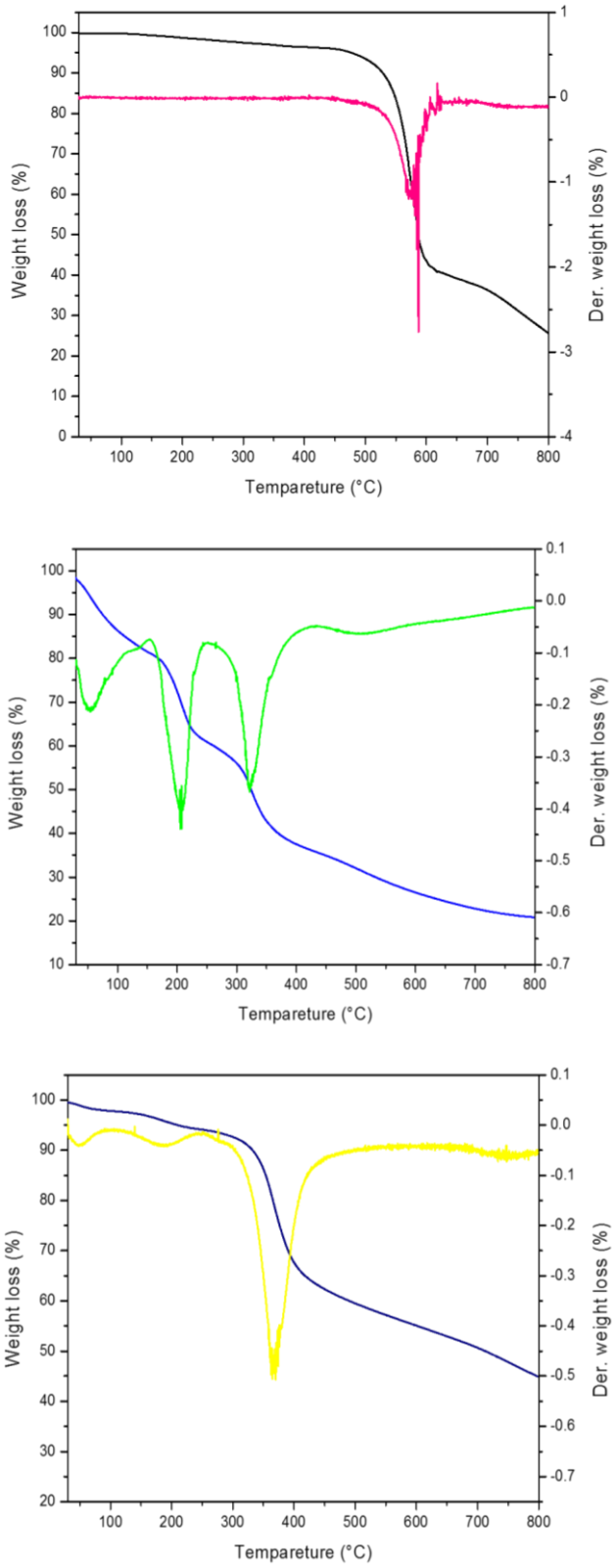

Fig. 5. TGA and DTG profiles of bare PES (a), PES-NO_2 (b) and Q-PES (c) materials.

The cloud points were measured and plotted in the ternary diagram as shown in Figure 7. The homogeneous solutions are positioned on the phase diagram in the region between the polymer/solvent axis and the precipitation and the precipitation curve in the ternary phase diagram. The tolerance of the system towards water before coagulation is indicated by the width of the region. The more water that can be added to the polymer blend casting solution, the more thermodynamically stable the casting solution is. A larger miscibility gap was assumed to result in instantaneous demixing in the coagulation bath, which leads to the formation of membranes with more

microvoids in the sublayer [21]. While increasing the polymer amount in the blend casting solution, less water was needed to cause precipitation. This implies that the casting solution was thermodynamically less stable. Boom and co-workers reported similar observations for the PES polymer system [22].

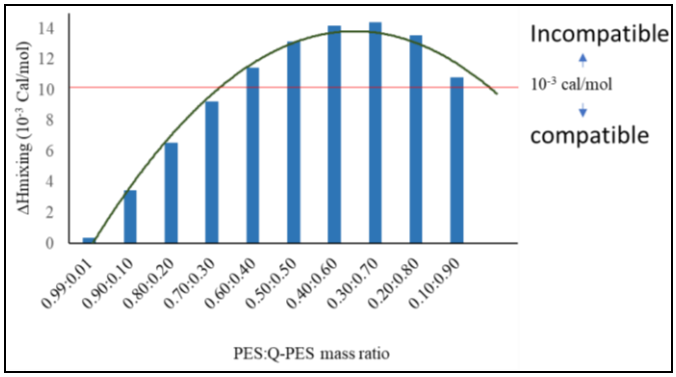

Fig. 6. The enthalpy of mixing of different ratios of PES/Q-PES blend systems. The polymer system is compatible when ΔH_m is below 10^{-3} cal/mol and incompatible beyond.

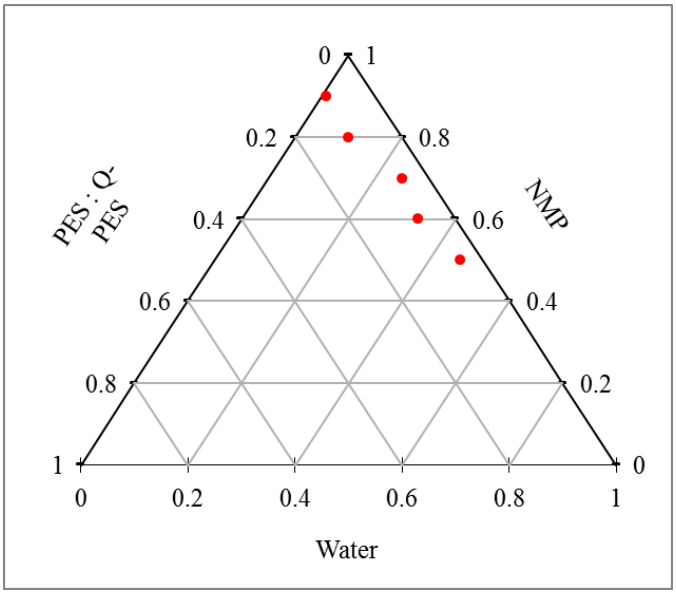

Fig. 7. Ternary phase diagram of PES: Q-PES-NMP-Water system.

3.3. Characterization of the membranes

3.3.1. Surface morphology of the membranes

Figure 8 shows three-dimensional AFM images of the membrane surfaces. In these images, the brightest area demonstrates the highest point of the membrane surface and the dark regions illustrate the valleys or voids or membrane pores. It is observed that the morphology of the surface of bare PES membrane (M1) charges when Q-PES was added into PES casting solution. It seems that the surface pores of the Q-PES/PES blend membranes were higher than that of the bare PES membranes, and this significantly increased with an increase in the amount of Q-PES into the PES casting polymer.

For quantitative analysis, the average roughness (S_a), the root mean square of the Z data (S_q) and the mean difference between the highest peaks and the lowest valleys (S_z) of the membrane surface were obtained from AFM images using project four software. These roughness parameters of the membranes are presented in Table 3, which were calculated in the AFM scanning area of 4 μm × 4 μm. The roughness of bare PES was lower than Q-PES membranes. M1 membranes had the lowest roughness, which increased with an increase in the ratio of Q-PES to PES polymer. As the amount of Q-PES increases, the light (white) peaks that indicate the hydrophobic regions gradually decrease and the deep brown peaks that represent the hydrophilic regions originating from the amine groups increase. Generally, the addition of Q-PES into PES casting solution increases the hydrophilicity of the membranes.

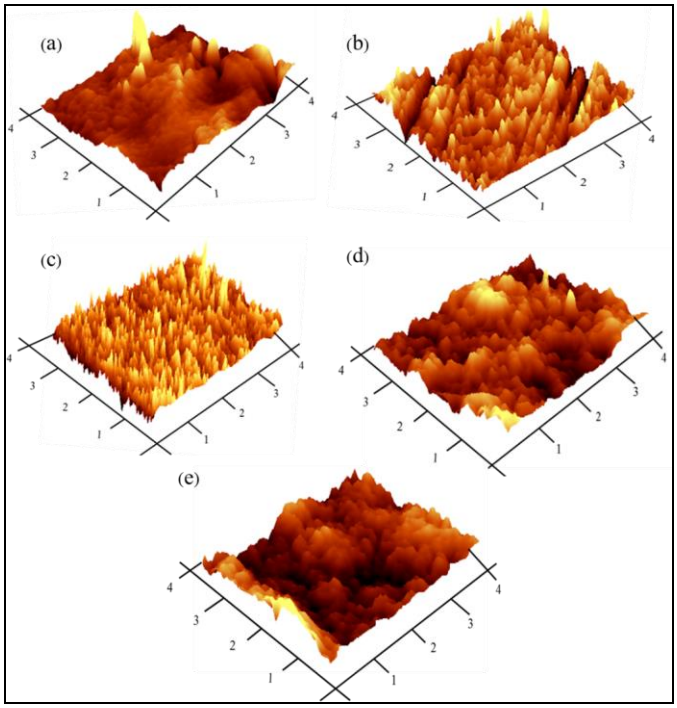

Figure 8. AFM images of different kinds of membranes synthesized using phase inversion: M0 (a), M1 (b), M2 (c), M3 (d) and M4 (e).

Table 3
Surface roughness of the membranes.

Membranes	S_a	S_q	S_z
M0	9.29	12.79	217.38
M1	49.33	71.25	975.25
M2	36.26	51.04	534.05
M3	33.76	63.12	789.92
M4	27.01	33.81	223.33

3.3.2. Charge density of the membranes

The surface charge of the bare PES and Q-PES are shown in Figure 9. The bare PES has slightly negatively charged surface throughout the tested pH value range, auto-titrated from a pH of 2 – 10. Constructively, the isoelectric points of the Q-PES membranes are in the pH range of 7.5 – 8. This indicates that these Q-PES membranes are positively charged below this pH range while they are negatively charging beyond this pH range. This was due to the presence of the ampholytic nature of amine groups on the structure of PES membranes. Furthermore, the higher the degree of amination, the higher the zeta potential readings and hence the higher the surface charge density of the membranes.

3.3.3. Contact angle measurements and surface free energy of the membranes

Contact angle measurements of different liquids were used to evaluate the kind and strength of the interactions across the solid/liquid interface. Furthermore, the hydrophilicity/hydrophobicity nature of the solid materials, membranes was investigated using contact angle measurements. The contact angles of water, glycerol, and DDM on the surface of membranes are shown in Figure 10.

For all the liquids, the contact angles of bare PES (M0) for all liquids were higher than that of Q-PES membranes, and the contact angles decreased (from 75.00±4.42º, 68.73±3.16º and 44.2±3.57º to 59.59±5.05º, 67.07±5.17º and 29.01±3.16º respectively for water, glycerol, and DDM) with an increasing ratio of Q-PES polymer added into the PES casting solution. This

implied that modification of PES by adding Q-PES improved the hydrophilicity of the membranes. The enhancement of the hydrophilicity of the membranes was attributed to the introduction of hydrophilic amine groups into the matrix of PES.

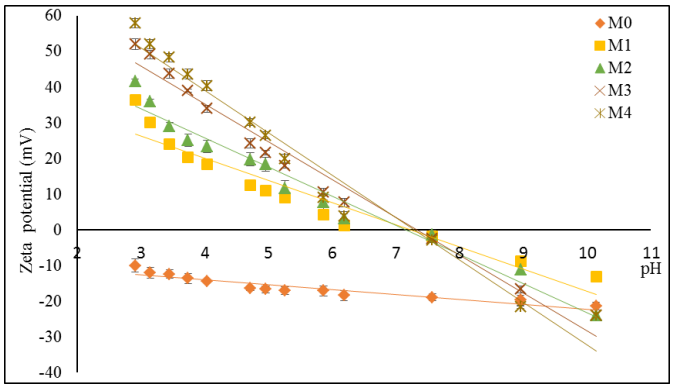

Fig. 9. Zeta potential measurements bare PES and aminated-PES systems at different pH level (pH 3-10).

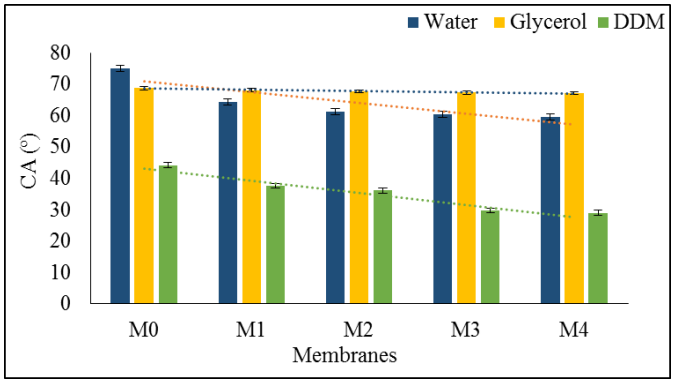

Fig. 10. Contact angle of water, glycerol, and DDM on bare PES an aminated-PES.

The amination modification of PES is accompanied by a change in surface energies. The Lifshitz van der Waals (γ_s^-) acid (γ_s^+) and basic (γ_s^-) of the surface tension were computed using the Oss-Chaudhary-Good thermodynamic approach by defining the contact angles [18]. The values of the surface tension and their components for water, glycerol, and DDM (Tables 4 and 5) [23], surface free energy components of PES and PES-blend system were calculated from experimental data for these liquids on the membrane surfaces with a considerable roughness and porosity. All the membranes have γ_s^+ values higher than γ_L^- and this meant that all the membranes exhibited a preponderant characteristic of a Lewis acid; hence, the membranes can be able to accept an electron. The Lewis acid can be explained in terms of a non-participant p orbital of nitrogen and oxygen atoms from the polymeric structure. The variation of γ_s^{AB}, γ_L^+ and γ_L^- with an increase in the amount of Q-PES to PES resulted in a charge of the polarity of the membranes, thus making them monoacidic, and hence the bipolar characteristics become more pronounced.

The total free energy surface of the membranes gradually decreases with an increase in the ratio of Q-PES added to the PES matrix solution (Figure 11). This implied that the hydrophilicity nature of the surface of the membranes was enhanced by the addition of the hydrophilic amine groups.

Table 4
The values of surface tension and their components for testing liquids (at room temperature).

Liquids	γ_L (mJ /m²)	γ_L^+ (mJ /m²)	γ_L^- (mJ /m²)	γ_L^{LW} (mJ /m²)
DDM	50.8	0	0	50.8
Glycerol	64	3.92	57.4	34
Water	72.8	25.5	25.5	21.8

Table 5
The values of surface free energy components of PES and aminated-PES calculated by acid-base approach.

Samples	γ_S^{LW} (mJ /m²)	γ_S^- (mJ /m²)	γ_S^+ (mJ /m²)	γ_S^{AB} (mJ /m²)
M0	49.71	1.16	39.15	13.48
M1	50.41	0.18	2.12	1.24
M2	10.81	3.12	3.05	6.17
M3	10.65	2.05	9.93	9.02
M4	0.85	5.93	10.57	15.83

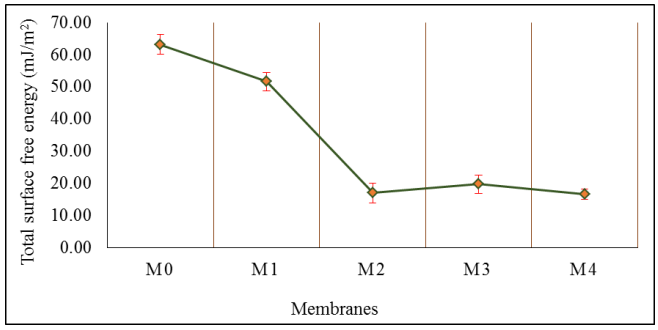

Fig. 11. The total surface free energy of PES and aminated-PES membranes calculated using Oss-Chaudhary-Good thermodynamic approach.

3.3.4. IEC, water uptake, thickness, strength, electrical resistance and conductivity parameters of the membranes.

Table 6 shows the influence of adding Q-PES into a PES matrix on the water content and IEC. The IEC increased with an increase in the amount of Q-PES added to PES while water uptake decreased. Membrane M0 possessed low IEC with the high-water uptake (80%), while membrane M4 possessed high IEC with low water uptake. M2 seemed to have both the IEC (0.163 mmol/g) and water uptake (58%) balanced. In general, an optimum water content is that which allows the best IEC, hence membrane M2 had the best water uptake with the best IEC. IEC and water uptake of the Q-PES membranes, especially M2 membranes were comparable to the commercial membranes, Fujifilm (Type 1) membranes.

As shown in Table 2, the thicknesses of the membranes were in the range of 94.46 – 95.23 µm, lower than that of the commercial membranes (2.40 MPa). The tensile strength decreased from 2.36 to 1.83 MPa when the amount of Q-PES was increased. When Q-PES was blended with PES, the formation of a hydrogen bond resulted in a compatible system. However, as more Q-PES was added to the PES matrix, there was formation of a cluster, not a bond; hence, the strength and compatibility were lost.

The electrical resistance is an important property of electromembrane processes due to its relationship with energy consumption. The membrane electrical resistance decreased sharply from 26.1 to 6.5 Ω cm^{-1} with an increase in the addition of Q-PES additives in the blend membrane. However, the conductivity of the membranes increased rapidly with an increase in the addition of Q-PES additive in the blend system. The low electrical resistance of Q-PES/PES blend anion exchange membranes was due to the formation of suitable ionic pathways in the membrane matrix by the introduction of amide functional groups, which in turn enhanced ion transport, thus lowering the areal electrical resistance.

4. Conclusions

PES-based blend membranes were prepared from PES/Q-PES using NMP as a solvent and water as coagulant *via* immersion precipitation phase inversion. The compatibility and properties of the PES-based blend system were affected by the addition of Q-PES. The PES/Q-PES blend system was compatible at the polymer ratio of 0.70:0.30 (PES:Q-PES) and below, thus resulting in a thermodynamically stable blend and delay in solvent-non solvent demixing, hence yielding membranes with uniformly distributed microvoids. Beyond the PES:Q-PES of 0.70:0.30, the blend system was incompatible, leading to thermodynamic instability and instantaneous demixing. The amine groups of Q-PES enhanced the IEC and water uptake,

while also improving the hydrophilicity of the membranes. The tensile strength of the membranes was compromised when larger quantities of Q-PES were added to the blend system. Q-PES improved the conductivity and electrical resistance of the blend membranes.

Acknowledgement

The authors are grateful for financial support from the University of South Africa and National Research Foundation (NRF) of South Africa. The work reported here is part of a joint-PhD project between the University of South Africa and Ghent University.

Table 6
IEC, water uptake, thickness, strength, electrical resistance and conductivity parameters of the membranes.

Membrane	IEC /mmol/g	Water uptake /%	Thickness /µm	Burst strength /MPa	Electrical Resistance/Ωcm^2	Conductivity /m Scm^{-1}
M0	0.15	79.07	95.23	2.36	26.00	36.54
M1	0.16	64.24	94.96	2.22	16.45	57.75
M2	0.16	55.42	95.16	2.09	13.88	68.45
M3	0.17	43.46	94.46	1.94	10.78	88.13
M4	0.17	39.88	94.77	1.83	6.45	147.40
Fujifilm AEM (Type 1)	0.16	50.46	125.00	2.40	8.00	156.25

NB: Fujifilm AEM (Type 1) is a commercial anion exchange membrane.

References

[1] M. Irfan, E. Bakangura, N.U. Afsar, M.M. Hossain, J. Ran, T. Xu, Preparation and performance evaluation of novel alkaline stable anion exchange membranes, J. Power Sources, 355 (2017) 171–180.

[2] S. Kwon, A.H.N. Rao, T.H. Kim, Anion exchange membranes based on terminally crosslinked methyl morpholinium-functionalized poly(arylene ether sulfone)s, J. Power Sources, In press, (2017) 1–12, 2017. Doi: 10.1016/j.jpowsour.2017.06.047.

[3] X. Luo, S. Holdcroft, Water permeation through anion exchange membranes, J. Power Sources, 355 (2017) 1–10.

[4] K. Emmanuel, C. Cheng, B. Erigene, A.N. Mondal, N.U. Afsar, M.I. Khan, M.M. Hossain, C. Jiang, L. Ge, L. Wu, T. Xu, Novel synthetic route to prepare doubly quaternized anion exchange membranes for diffusion dialysis application, Sep. Purif. Technol. 189 (2017) 204–212.

[5] W. Mei, Z. Wang, J. Yan, Poly(ether sulfone) copolymers containing densely quaternized oligo(2, 6-dimethyl-1, 4-phenylene oxide) moieties as anion exchange membranes, Polymer 125 (2017) 265–275.

[6] H. Abdul Mannan, H. Mukhtar, M. Shima Shaharun, M. Roslee Othman, T. Murugesan, Polysulfone/poly(ether sulfone) blended membranes for CO_2 separation, J. Appl. Polym. Sci. 133 (2016) 1–9.

[7] W. Cui, J. Kerres, G. Eigenberger, Development and characterization of ion-exchange polymer blend membranes, Sep. Sci. Technol. 14 (1998) 145–154.

[8] J. Yan, H.D. Moore, M.R. Hibbs, M.A. Hickner, Synthesis and structure-property relationships of poly(sulfone)s for anion exchange membranes, J. Polym. Sci. Part B: Polym. Phys. 51 (2013) 1790–1798.

[9] X. Liao, L. Ren, D. Chen, X. Liu, H. Zhang, Nanocomposite membranes based on quaternized polysulfone and functionalized montmorillonite for anion-exchange membranes, J. Power Sources, 286 (2015) 258–263.

[10] E.A. Weiber, P. Jannasch, Ion distribution in quaternary-ammonium-functionalized aromatic polymers: effects on the ionic clustering and conductivity of anion-exchange membranes, ChemSusChem. 7 (2014) 2621–2630.

[11] C. Manea, M. Mulder, Characterization of polymer blends of polyethersulfone/ sulfonated polysulfone and polyethersulfone/sulfonated polyetheretherketone for direct methanol fuel cell applications, J. Membr. Sci. 206 (2002) 443–453.

[12] B. Schneier, Polymer Compatibility, J. Aplied Polym. Sci. 17 (1973) 3175–3185.

[13] A.K. Ho, B. Aernouts, W. Saeys, I.F.J. Vankelecom, Study of polymer concentration and evaporation time as phase inversion parameters for polysulfone-based SRNF membranes, J. Membr. Sci. 442 (2013) 196–205.

[14] M. L. Masheane, L.N. Nthunya, S.P. Malinga, E.N. Nxumalo, B.B. Mamba, S.D. Mhlanga, Synthesis of Fe-Ag/f-MWCNT/PES nanostructured-hybrid membranes for removal of Cr (VI) from water, Sep. Purif. Technol. 184 (2017) 79–87, 2017.

[15] Q. Zhang, H. Wang, S. Zhang, L. Dai, Positively charged nanofiltration membrane based on cardo poly(arylene ether sulfone) with pendant tertiary amine groups, J. Membr. Sci. 375 (2011) 191–197.

[16] E. Chibowski, On some relations between advancing, receding and Young's contact angles, Adv. Colloid Interface Sci. 133 (2007) 51–59.

[17] M. Jurak, Surface free energy of organized phospholipid/lauryl gallate monolayers on mica, Colloids Surfaces A: Physicochem. Eng. Asp. 510 (2016) 213–220.

[18] C. J.V.A.N. Oss, M. K. Chaudhuty, R. J. Good, Interfacial Lifshitz-van der Waals and polar interactions in macroscopic systems, Chem. Rev. 88 (1988) 927–941.

[19] W. Wu, R.F. Giese, C.J. van Oss, Evaluation of the Lifshitz-Van Der Waals acid-base approach to determine surface-tension components, Langmuir 11 (1995) 379–382.

[20] W. Chen, X. Yan, X. Wu, S. Huang, Y. Luo, X. Gong, G. He, Tri-quaternized poly (ether sulfone) anion exchange membranes with improved hydroxide conductivity, J. Membr. Sci. 514 (2016) 613–621.

[21] K. Hendrix, M. Vaneynde, G. Koeckelberghs, I.F.J. Vankelecom, Synthesis of modified poly (ether ether ketone) polymer for the preparation of ultra filtration and nano filtration membranes via phase inversion, J. Membr. Sci. 447 (2013) 96–106.

[22] R. Boom, T. van den Boomgaard, J.W.A. van den Berg, C.A. Smolders, Linearized cloud point curve corelation for ternary systems consisting of one polymer, one solvent and one non-solvent, Polymer 34 (1993) 2348–2356.

[23] M. Florea-spiroiu, M. Olteanu, V. Stanescu, G. Nechifor, Surface tension components of plasma treated polysulphone membranes Chimie, Anul XVII (serie nouă) 2 (2008) 13–18.